

Hybrid PVDF/PANI Membrane for Removal of Dyes from Textile Wastewater

Hifza Nawaz, Muhammad Umar, Iqra Nawaz, Azeem Ullah, Muhammad Tauseef Khawar, Marek Nikiel, Humaira Razzaq, Muhammad Siddiq, and Xuqing Liu*

Treatment of textile wastewater has been a matter of considerable interest because of the potential toxicity, colloidal stability, and deformable nature of dyes. Herein, a novel polyaniline (PANI)/polyvinylidene fluoride (PVDF) hybrid membrane is developed to remove textile wastewater dyes. The hybrid membrane's contact angle decreases by increasing the concentration of polyaniline in the PVDF matrix, enhancing the hybrid membrane's hydrophilicity. Membrane properties, including porosity, antifouling property, solvent content, and pure water flux, are improved in the hybrid membrane compared with neat PVDF membranes. The purified water flux is enhanced from 28 to 47 L m⁻² h, which indicates the impact of PANI on the hydrophilicity of the hybrid membranes. Among the hybrid membranes, 3P exhibits 85% dye rejection at 0.1 MPa operating pressure. Hence, the incorporation of PANI in the PVDF matrix is proposed to enhance the hybrid membrane's dye rejection and antifouling properties.

the Earth's surface and serves as a critical component for the human body and other living organisms. These facts show the essential relation of human health with water and the ecosystem. The provision of clean water is necessary for every human being and their growth.^[1] Wastewater released from the textile industry is one of the extensive sources of pollution for water and soil. For the protection of aquatic ecosystems, harmless treatment has tremendous importance in textile wastewater treatment. Wastewater from textile industries containing fixed and unfixed dyes without appropriate treatment causes numerous problems in the nearby water resources.^[2] The major problem associated with textile wastewater is increased color concentration, leading to the reduction of

light transmittance in water, limiting aquatic life growth.^[3]

Purification of textile wastewater by conventional methods includes ozonation, bleaching, hydrogen peroxide treatment/UV treatment, and electrochemical techniques.^[4] One of the significant problems associated with these techniques is that they cannot decompose complex aromatic molecular structures that are stable toward light and oxidizing agents.^[5] However, several modern methods used to reduce the contamination in textile wastewater from the industries include biological and physiochemical processes.^[6] The problem with biological processes is that they cannot wholly remove the adverse effects of dyes and cause problems for the aquatic life and aquatic ecosystem. The other method includes the addition of certain compounds that leads to secondary pollution.^[7] Scientists and engineers are working to introduce more efficient methods for removing dyes from textile wastewater. In this context, pressure-driven membrane technology is getting much attention as it offers a cleaner, more convenient, and energy-efficient method for dye removal.^[8] These include ultrafiltration (UF), nanofiltration (NF), and reverse osmosis (RO). UF had been used to recycle high-molecular-weight compounds, insoluble dyes (e.g., indigo and disperse), and auxiliary chemicals. UF is now used as a pre-treatment step to reduce contamination by suitable pore sizes before treating NF and RO.^[9] UF is used for color filtration, but it cannot remove dyes and compounds with low molecular weight.^[10]

Mostly polyvinylidene fluoride (PVDF)^[11] is used for the fabrication of UF membranes due to its excellent properties such as good film-forming ability, mechanical strength, high thermal

1. Introduction

The pollution of the ecosystem, including air, water, and soil, is a severe concern in this current world. Water contributes to 78% of

H. Nawaz, M. Umar, M. Tauseef Khawar, M. Nikiel, X. Liu
Department of Materials
University of Manchester
Oxford Road, Manchester M13 9PL, UK
E-mail: xuqing.liu@manchester.ac.uk

I. Nawaz
Nuclear Institute for Agriculture and Biology
Pakistan Institute of Engineering and Applied Sciences
Jhang Road, Faisalabad 38000, Pakistan

A. Ullah
Nano Fusion Technology Research Group
Institute for Fiber Engineering (IFES)
Interdisciplinary Cluster for Cutting Edge Research (ICCER)
Shinshu University
Matsumoto, Nagano 390-8621, Japan

H. Razzaq, M. Siddiq
Department of Chemistry
Quaid-i-Azam University
Islamabad 45320, Pakistan

 The ORCID identification number(s) for the author(s) of this article can be found under <https://doi.org/10.1002/adem.202100719>.

© 2021 The Authors. Advanced Engineering Materials published by Wiley-VCH GmbH. This is an open access article under the terms of the Creative Commons Attribution License, which permits use, distribution and reproduction in any medium, provided the original work is properly cited.

DOI: 10.1002/adem.202100719

stability, excellent aging resistance, and chemical stability. Zheng et al.^[11] prepared a PVDF membrane, which has remarkable rejection for reactive dyes. For textile wastewater treatment, PVDF-based membranes have been gaining significant attention for their excellent separation performance. Wu et al.^[12] reported pure PVDF membranes for filtration of reactive red dye from textile wastewater and found that the pure water flux of membrane was 12–50 L m⁻²h⁻¹ and retention of dye was about 77–94%. Malaisamy^[13] prepared polysulfide composite membranes that can degrade brilliant green by the adsorption process from contaminated water. He et al. reported a combined method based on blending and photoreduction to synthesize the PVDF/TiO₂/Ag composite membrane that has shown high antibacterial activity as tested through the inactivation of bacteria under the illumination of visible light.^[14]

In the past few years, most researchers have modified the membrane's surface to increase its hydrophilicity.^[15] Modifications on the surface of the membrane were done using different techniques such as grafting, plasma, and blending with other hydrophilic polymers or nanoparticles that show excellent results.^[16] The polymer blend is one of the easy methods to improve membrane separation properties, among others. Yan et al.^[17] reported that membrane blending is a cost-effective method for membrane modification. Polyaniline (PANI)^[18] offers suitable substitutes for hydrophilic characteristics within the synthesized membrane because of its specific properties such as good steric hindrance, excellent adsorption capacity, easy preparation, and different functional groups for chemical interactions with PVDF during the process of membrane casting.

Our research article mainly focuses on the design of hybrid membranes to remove dye molecules from contaminated water. For this purpose, we synthesized the pure PVDF and PANI/PVDF hybrid filtration membranes through the phase-inversion process. A series of characterizations such as scanning electron microscopy (SEM), tensile strength, X-ray diffraction (XRD), thermogravimetric analysis (TGA), and Fourier-transform infrared spectroscopy (FTIR) was done to check the properties of the hybrid membrane. Permeation properties (shrinkage ratio, porosity, pure water flux, solvent content, and bovine serum albumin [BSA] rejection) of PVDF/PANI membranes were investigated to check the performance of synthesized membranes in water purification.

2. Experimental Section

2.1. Materials

Chemicals PVDF (Alfa Aesar), PANI (polyaniline) with the molecular weight of 10 000 g mol⁻¹ (Sigma-Aldrich), *N,N*-dimethyl formamide (DMF) synthesis grade 97% (scharlu), 1-propanol (99.09%) (Alfa Aesar), ethanol (≥99.07%) (scharlu), sodium hydroxide (NaOH, ≥97%) (Alfa Aesar), and acetic acid (CH₃COOH, ≥99%) were used as received.

2.2. Fabrication of PVDF–PANI Hybrid Membranes

Hybrid PVDF membranes were synthesized by adding PANI (1–4 wt%) to enhance the PVDF membrane's hydrophilicity.

The 3% w/v polyaniline was found to be best for membrane preparation and filtration processes. By further increasing the PANI percentage, the synthesized membrane became brittle and broke during the drying process, so it could not be used for characterization and application processes. PVDF (11–15 wt%) and PANI (1–4 wt%) were solubilized in DMF solvent at 59 °C under constant stirring for 24 h to prepare a homogenous solution. Both PVDF and PANI were organic polymers in nature and readily miscible. Degassing was conducted by keeping the membrane's casting solution in a vacuum oven for 1 h at 40 °C. The clear solution was spread on a glass plate substrate with a hand-casting knife, and then it was directly dipped into the coagulation bath, which contained deionized water at 25 °C.^[12] For extraction of remaining solvents in the synthesized PVDF/PANI hybrid membrane, the shaped membrane was kept in fresh distilled water for 24 h. **Figure 1** shows the membrane manufacturing process by phase-inversion technique.

The codes and compositions for different membrane samples are shown in **Table 1**.

2.3. Characterizations

Synthesized membranes were characterized for structural and morphological analysis by SEM, XRD, FTIR, and TGA. XRD (Panalytical 304/60 expert PRO) in the range from 5° to 80° was used to evaluate membrane samples' structural characteristics. For identifying functional groups of hybrid membranes, FTIR analysis was done within the range of 400–4000 cm⁻¹. The thermal stability of synthesized membranes was calculated by TGA (PerkinElmer, USA). SEM (VP-1450 Germany, LEO) was used to determine the cross-sectional area and surface morphology of the synthesized water purification membranes. Further, ImageJ software was used for the geometric analysis of the synthesized membrane.

3. Permeation Properties of the Synthesized Membrane

3.1. Porosity

To measure the porosity of synthesized membranes, they were cut to 1 cm² pieces and then dipped into deionized water for 24 h. We measure the weight of the membrane's pieces before and after submerging into water. The value of porosity was calculated using the following formula.^[19]

$$\text{Porosity \%} = \frac{W_2 - W_1}{A_h} \times 100 \quad (1)$$

A_h represents the cross-sectional area of membranes, W_1 is the weight of the dry membrane, and W_2 is the wet membrane's weight.

3.2. Solvent Content

To determine solvent content of the synthesized membranes, the membranes were cut into small pieces of 1 cm² and then dipped into various solvents, that is, ethanol, water, propanol, and

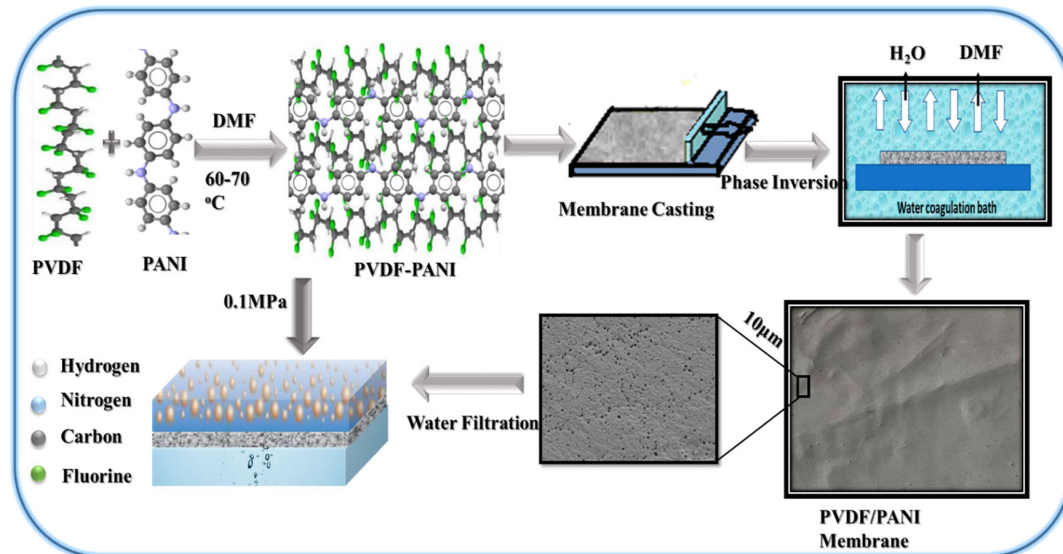


Figure 1. A schematic representation of membrane manufacturing process.

Table 1. Code of PVDF/PANI hybrid membranes.

Code	PVDF [w/v %]	PANI [w/v %]	DMF [w/v %]	Total conc. [w/v %]
0P	15	0	85.0	100
1P	14	1	85.0	100
2P	13	2	85.0	100
3P	12	3	85.0	100
4P	11	4	85.0	100

methanol. We measured the weight of dry and wet membranes after immersing in the earlier solvents. Solvent content was calculated using the following formula.^[20]

$$\text{Solvent Content \%} = \frac{W_2 - W_1}{W_2} \times 100 \quad (2)$$

W_1 is the weight of the dry membrane, whereas W_2 is the weight of the wet membrane.

3.3. Pure Water Flux

Pure water flux was measured to check the performance of synthesized membranes in water purification. First, the membranes were immersed in distilled water for 30 min. A vacuum pump was used for measuring the water flux at 0.1 MPa.^[21] The value of pure water flux was calculated using the following equation.

$$\text{Pure Water Flux (J)} = Q/At \quad (3)$$

where “A” represents the area of the membrane (cm²) and “Q” the amount of water that passes through the membrane in time “t.”

3.4. Membrane Shrinkage

A small piece of the membrane was dipped into distilled water for 12 h. Length and width were measured before and after dipping it in water through a screw gauge and vernier caliper. The value of the shrinkage ratio was calculated using the following formula^[22]

$$\text{Shrinkage ratio \%} = \left[1 - \frac{(a \times b)}{(a_o \times b_o)} \right] \times 100 \quad (4)$$

a_o and a represent the length of wet and dry membranes, whereas b_o and b show the thickness of wet and dry membranes, respectively.

3.5. Antifouling Properties

BSA solution was used to check the antifouling properties of the hybrid membrane. It is a model fouling protein used to investigate antifouling characteristics of the synthesized membrane. Initial water flux (J_{w1}) was measured using BSA (0.8 g L⁻¹) solution in the filtration cell. After filtration, the fouled membrane was washed by dipping it into distilled water for 30 min at 25 °C. Further, the pure water flux (J_{w2}) was again measured. Flux recovery ratio was calculated using the following formula.

$$\text{FRR \%} = \frac{J_{w1}}{J_{w2}} \times 100 \quad (5)$$

The following formula was used for measuring the value of BSA rejection.

$$\% R = \left(1 - \frac{C_p}{C_f} \right) \times 100 \quad (6)$$

C_f and C_p represent the value of molarity of feed and permeate solutions.

A UV-vis spectrophotometer was used to analyze the molarity of permeate and feed of BSA^[19] solution ($\lambda_{\text{max}} = 280 \text{ nm}$).

3.6. Experiments for Adsorption Process

We conduct all experiments with Erlenmeyer flask (250 mL) under continuous stirring at 298 K temperature. We optimized our results with pure PVDF and PVDF/PANI membrane. To check the membrane's adsorption capacity, we dipped the $0.5 \times \text{g}$ developed membrane into 100 L^{-1} dye solution at 6.5 pH, 298 K, and a continuous temperature at 100 rpm. Dye contamination was measured by UV-vis spectroscopy. We also measure the different parameters such as membrane concentrations, pH, and time through adsorption experiments.

The following formula was used to measure the value of adsorption (q_e).

$$\text{Adsorption } (q_e) = \frac{(C_0 - C_e)V}{m} \quad (7)$$

We used 0.01 M NaOH and 0.01 M HNO₃ to adjust the value of pH. To study the kinetic adsorption isotherm, we dipped $0.6 \times \text{g}$ of synthesized membranes into a different concentrated solution of methylene orange.

4. Results and Discussion

4.1. Morphology of Membrane

Surface morphologies of synthesized membranes and polyaniline effects on membrane's surfaces were investigated by SEM analysis. **Figure 2** (A1–D1) shows SEM micrographs of hybrid membranes that contain 1% w/v, 2% w/v, and 3% w/v concentrations of polyaniline as hydrophilic polymers and pure PVDF membrane. According to the SEM image, the content of polyaniline improves the surface roughness of our developed membranes. The surface of the membrane also shows a pit-like structure. The number of pores within hybrid membranes increases, which enhances pure water flux and hydrophilicity of hybrid membranes. To investigate the structure and size of pores, we conducted geometric analysis of SEM images using ImageJ software, which shows that the number of pores on the membrane surface increased. Still, the size of pores gradually decreases with an increase in polyaniline concentration.^[23] The estimated diameter and distributions of the membrane's pores are shown in **Figure 2A2–D2**. We observed that the synthesized PVDF membrane contains fewer pores on the surface, whereas the hybrid membranes have increased number of pores with increasing polyaniline content.^[24] The average diameter of pores for the hybrid PVDF/PANI membrane is around $0.78 \mu\text{m}$, whereas the pure PVDF membrane's diameter is about $1.53 \mu\text{m}$. This reduction in the hybrid membrane's pores' diameter is evidence of complex structure formation due to its excellent chemical interactions between polyvinylidene fluoride and polyaniline.

The cross-sectional images of synthesized membranes are shown in **Figure 2A3–D3**. Results show that developed membranes have good polymer compatibility and do not display any phase separation. The cross-sectional images show the

asymmetric morphology of the synthesized membrane. The thickness of synthesized membranes was about $100\text{--}150 \mu\text{m}$. SEM images of neat PVDF membrane (A) show compact layer on the upper side and asymmetric structure of pores within the membrane. This thick layer on the top surface was due to the quick phase-inversion process into a coagulation bath. Hybrid PVDF/PANI membranes show a more porous structure with uniform distribution of pores throughout the membrane.^[25]

4.2. Surface Composition of PVDF/PANI Membranes

XRD analysis represents diffractograms of PVDF and PVDF-PANI hybrid membrane with varying PANI amounts from 1% to 3% in the range of $10^\circ\text{--}80^\circ$, as shown in **Figure 3a**. In the XRD pattern, PVDF has three crystalline phases α , β , and γ . Among these three phases, β and γ are polar, whereas the α -phase is nonpolar. The PVDF has 2θ values of 18.4° and 19.6° , which correspond to the α -phase of PVDF. For wastewater treatment applications, the polar phase in hybrid membranes is useful. The XRD spectra show a phase change from nonpolar to polar after 1–3% w/v of PANI in the hybrid membrane.^[26] The peak intensity of α -phase at 18.4° slowly decreased and became invisible with addition and increasing polyaniline concentration. However, a more intense peak at 20.2° was observed. This peak is attributed to the stabilization of the β -crystalline phase of the PVDF in the hybrid membrane. The intensity of peaks at 20.2° and 39.0° was also slightly increased by the addition of PANI, and the area under the peak at 20.2° broadened in hybrid membranes. XRD results conclude that developed hybrid membranes represent enhanced polar β -crystalline phase. When the polar phase within the hybrid membrane increases, then these membranes also exhibit enhanced hydrophilic nature.^[27] FTIR analysis was done for the determination of additives (polyaniline) that persisted or infiltrated into the coagulation bath during the synthesis of hybrid membranes, FTIR spectra of unadulterated PVDF and mixture PVDF/PANI layers at three fixations (1, 2, 3% w/v) are shown in **Figure 3b**. The trademark crests of PVDF can be seen in all membranes. C–F stretching vibrations of PVDF were assigned at the wavenumber 1022 cm^{-1} , the ridge at 1232 cm^{-1} is compared with the –C–H group in protonation. The peak intensity at around 1359 cm^{-1} for N–H bending increases upon the addition of PANI. The peak at 844 cm^{-1} is because of the aromatic ring present in polyaniline. The quinoid and benzenoid rings of PANI appear at around 739 cm^{-1} . The peak at 1537 cm^{-1} corresponds to the benzenoid ring's C–N stretching at 1537 cm^{-1} .^[28]

TGA was used to study the thermal behavior of the pure and hybrid membranes. TGA of hybrid membranes with variable concentrations of PANI, that is, from 1 to 3 wt%, is shown in **Figure 3c**. At the TGA operating temperature from 35 to 800°C , the pure PVDF membrane showed higher weight loss than the hybrid membranes. The hybrid membranes showed increased thermal decomposition (Td) between 405 and 468°C .^[29] This increase in Td validates the hybrid membranes' thermal stability. It establishes that the hybrid membranes' thermal stability will increase as the concentration of PANI increases from 1% to 3%.^[30] The degradation temperature also increased due to the good interfacial interactions between the PANI and the

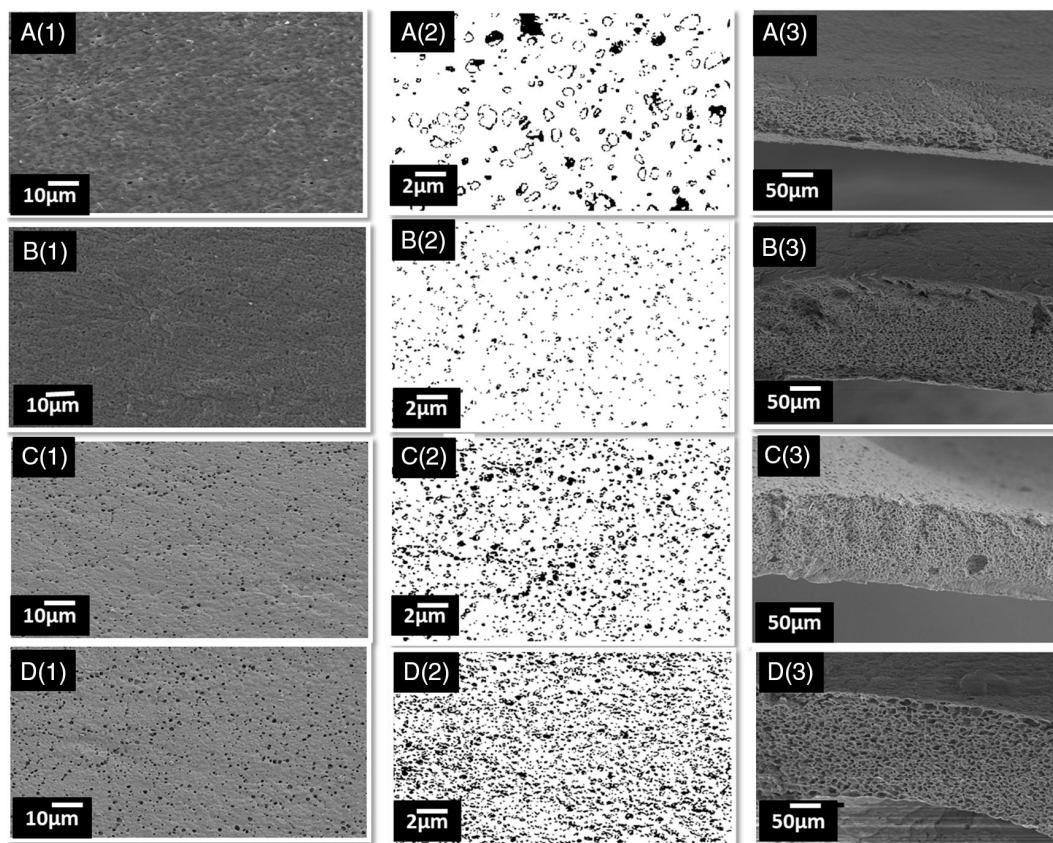


Figure 2. A1) Morphology of membrane surface. A2) Pores geometry. A3) Cross-sectional images of pure PVDF membrane. B1) Morphology of membrane surface. B2) Pores geometry. B3) Cross-sectional images of 1P hybrid membrane. C1) Morphology of membrane surface. C2) Pores geometry. C3) Cross-sectional view of 2P hybrid membrane. D1) Morphology of membrane surface. D2) Pores geometry. D3) Cross-sectional images of the 3P hybrid membrane.

PVDF. PVDF is a flexible plastic polymer, and in the tensile stress–strain curve, it shows a typical ductile behavior associated with chain mobility beyond elastic limit upon applied stress. Figure 3d shows the stress–strain profile of neat PVDF and hybrid PVDF/PANI membrane. As evident from the results, the increase in PANI concentration increases the hybrid membranes' mechanical strength. The mechanical performance of PVDF/PANI hybrid membranes increased due to the right chemical interactions between polymers (PANI and PVDF).^[31] Young's modulus increases from 45.01 to 90.21 MPa with PANI content, as shown in Table S2, Supporting Information. Similarly, the polymer membrane's tensile strength increased with an increase in PANI content in the hybrid membrane because polyaniline forms adjacent bonding structure with PVDF molecules that reduce pore size and increase their mechanical strength. Elongation at break also shows an increasing trend due to the decrease in hydrogen bonding.^[32]

4.3. Permeation Studies of the PVDF/PANI Hybrid Membranes

Contact angle measurements determined the hydrophilicity of the membrane's surface. During the filtration process, air is filled within the porous structure of the membrane. It directly

affects the contact energy of water droplets, which varies the value of contact angle. This effect of porosity on contact angle can be explained through Cassie–Baxter's model.

$$\cos \theta = P \cos \theta_p + (1 - P) \cos \theta_{np} \quad (8)$$

Here θ_p is the contact angle of the porous portion, whereas θ_{np} is the contact angle of nonporous part of the developed membrane. P is the measured porosity of developed membranes. Cassie–Baxter's model gives the value of contact angle of porous portion and rough surface area of nonporous portion. It shows that the area of the liquid–solid interface declines when the value of water contact angle increases. This is due to increase in surface roughness (as shown in SEM images), which reduces the adhesion between droplet and membrane surface and decreases the area of liquid–solid interface.^[33] A decrease in contact angle leads to an increase in the hydrophilic property of the membrane. In this experiment, the contact angles of pure PVDF and PVDF/PANI membranes were investigated to compare the effect of the addition of various concentrations of PANI (1, 2, 3% w/v). Figure 4a shows that the addition and increase in PANI concentration led to the decreased contact angle of membrane surface due to the hydrophilic nature of PANI. PVDF is inherently hydrophobic; the –NH group in PANI results in hydrogen bonding

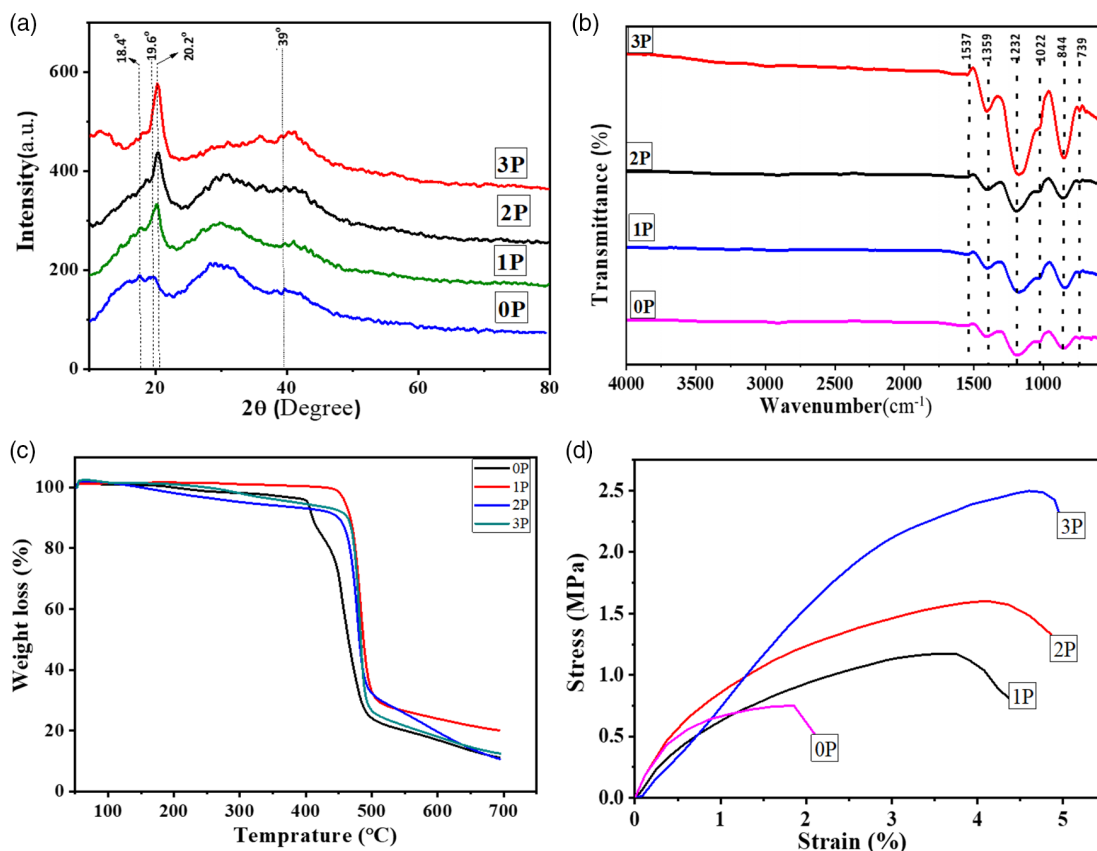


Figure 3. a) XRD, b) FTIR, c) TGA, and d) tensile results analysis of PVDF/PANI hybrid membranes with different concentrations of PANI.

with water molecules, thus imparting hydrophilicity to the hybrid membranes.^[34] The addition of PANI in the membrane casting solution results in an increased number of pores. It can be due to three main reasons; first, the membrane casting solution's viscosity decreases with increased PANI concentration. The diffusional exchange rate of solvent accelerates with a decrease in the casting solution's viscosity and increases the number of pores in PVDF/PANI hybrid membranes. The second reason is polyaniline, which acts as the hydrophilic polymer in the synthesis of the membrane. The third reason is the reduced compatibility of PVDF and PANI. The membrane porosity measurements are shown in Figure 4b. Porosity acts as an essential factor in membrane shrinkage properties. The higher the porosity, the lesser the percent shrinkage ratio. Graphical results of the percent shrinkage ratio are shown in Figure 4b. From the figure, unmistakably, the percent shrinkage proportion diminished continuously with an increment in polyaniline fixation. The shrinkage proportion is under 60% in these membranes, which is more effective for filtration.^[35]

The performance of the synthesized membrane in water purification was measured by calculating their solvent content. Different solvents in polarity from propanol to water were selected to determine the solvent absorption capacity of the hybrid membrane.^[36] The value of solvent contents was calculated by measuring the difference between the weight of dried and wet

membranes. After investigation of solvent contents of membranes, the results are shown in Figure 4c. These results indicate that polyaniline increased the hydrophilic characteristic,^[37] increasing the hybrid membrane's permeation properties by attracting the water molecule inside or outside the membrane surface.^[38] However, the hybrid membrane decreases the adsorption capacity for solvents of lower polarity (propanol < ethanol < methanol).^[39] Pure water flux was calculated to measure the water permeability of hybrid membranes at 0.1 MPa.^[40] Figure 4d shows that the pure water flux of PVDF/PANI membrane dramatically improved with increasing polyaniline concentration due to its hydrophilic properties.

4.4. Possible Mechanism of Dye Rejection and Effect of Dye Concentration

Two different types of dyes (allura red and methyl orange) were used to make 100 ppm solutions in distilled water to study dye rejection properties of synthesized membranes. **Figure 5** shows the water filtration property of pristine PVDF (0P) and PVDF/PANI hybrid membrane (1P, 2P, and 3P). The dye solutions were passed through synthesized membranes at a pressure of 0.1 MPa. Synthesized membranes have dye rejection capacity because of their sieving mechanism and adsorption behavior.^[41] The ability of dye rejection through membranes directly depends

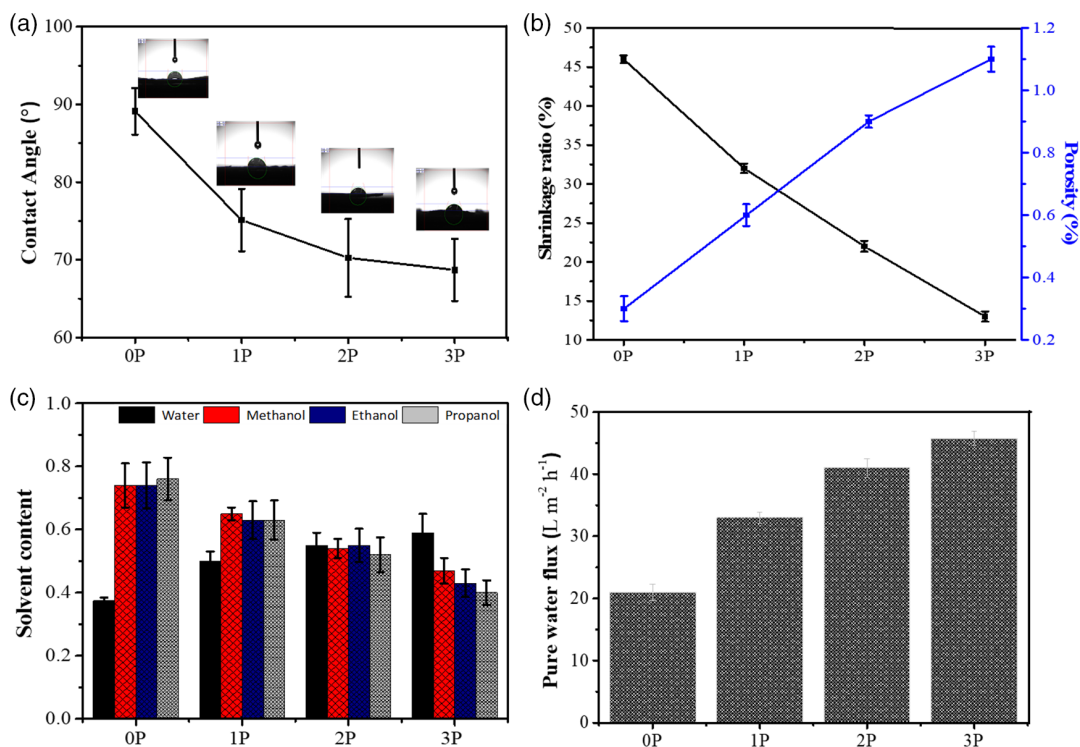


Figure 4. a) Graphs for contact angle. b) Shrinkage ratio and porosity. c) Solvent content. d) Water flux of PVDF-PANI hybrid membranes with different concentrations of PANI.

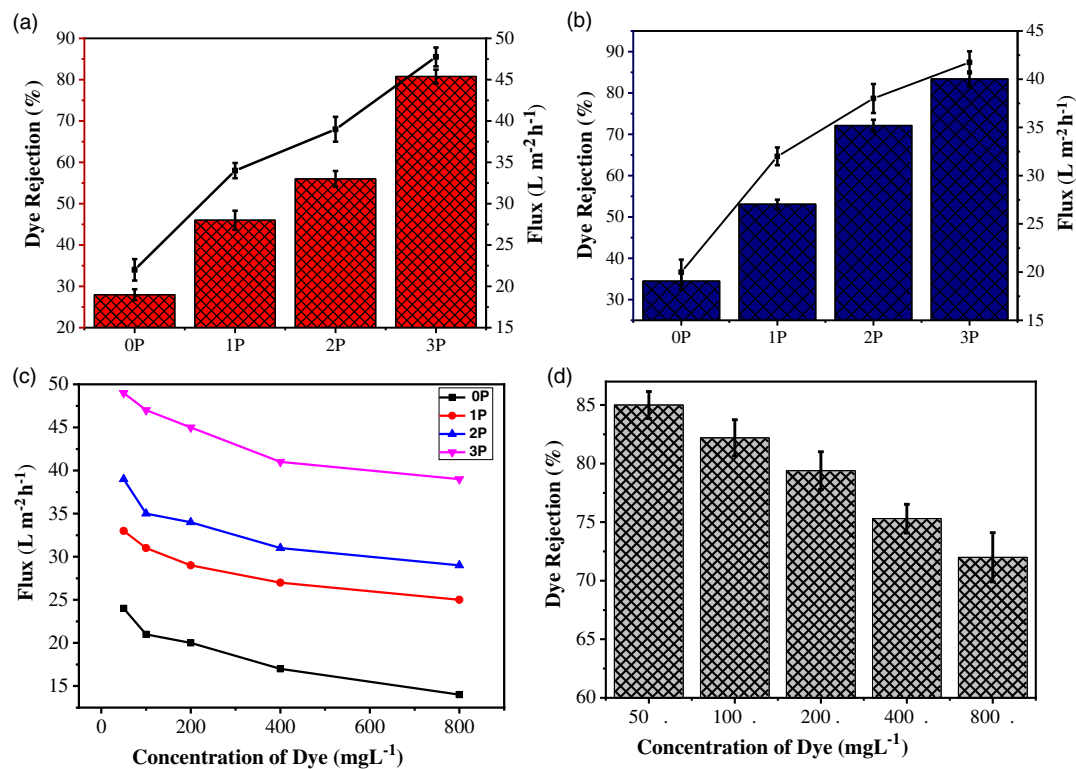


Figure 5. a) Dye rejection (allura red) and flux of PVDF/PANI hybrid membranes. b) Dye rejection (methyl orange) and flux of PVDF/PANI hybrid membranes. c) Effect of dye concentrations on flux. d) Effect of dye concentration on dye rejection of the hybrid membrane.

upon the molecular weight of dye molecules. Here we used the same membrane for the filtration of two different dye solutions to check their performance. Results show that the rejection rate of synthesized membranes increased for high molecular weight.^[42] Figure 5a,b shows that highly concentrated polyaniline membrane (3P) shows good performance for removal of dye molecules as compared with low-concentrate polyaniline membranes (1P and 2P) and neat PVDF membranes. The pore size of 3P membrane was less (about 0.78 μm) than the diameter of the dye molecule. Due to this, hybrid membranes show the sieving mechanism and restrict dye molecule flow through the membrane. Results show that the dye flux of synthesized PVDF membranes is less (about 23 $\text{L m}^{-2} \text{h}$) than that of hybrid membranes (1P, 2P, and 3P). Figure 5 shows that the removal efficiency of methyl orange was less than allura red due to its low molecular weight (327.33 g mol^{-1}) in comparison with allura red (496.42 g mol^{-1}).^[43]

According to the Film theory equation, the concentration of dyes in feed solution directly affects the filtration performance of synthesized membranes.^[44] To determine their effect on membrane flux and rejection efficiency, we prepared five solutions (50, 100, 200, 400, 800 ppm) with different methyl orange concentrations. According to Figure 5c, the dye flux of synthesized membranes was greatly affected by increasing the dye concentration in feed solutions. With increasing dye molecule concentration, the osmotic pressure on the membrane surface increased due to dye molecules' accumulation and deposition effect. Flux gradually declined with increasing concentration of the dye (from 50 to 800 ppm) in the feed solution. As the dye concentration increases, dye molecules deposit and aggregate onto the membrane's surface that cause a polarization effect and increased osmotic pressure within the membranes.^[45] The aggregate of dye molecules blocks the pores of the synthesized membrane, which causes membrane fouling. So, the dye fluxes of 0P, 1P, 2P, and 3P were decreased by 44%, 15.9%, 12.1%, and 10.2%, respectively. A highly concentrated polyaniline hybrid membrane shows good antifouling properties. Therefore it offers a significantly less decrease in dye flux.^[46] According to Figure 5d, the dye rejection rate was greatly affected by the increased dye concentration of feed solutions. Overall, the performance of synthesized hybrid membranes (3P) was less affected by increased dye concentration and good efficiency of dye rejection (84%). The experiment was conducted three times to check the reproducibility, and mean result values were displayed with their standard deviations.

The capacity of methyl orange adsorption through synthesized PVDF and PVDF/PANI membranes is shown in Figure 6a. All blends (PVDF/PANI) show better adsorption capacity than the pure PVDF membrane within order pristine PVDF (3.4%) < 1P (45%) < 2P (64.2%) < 3P (80%). We conducted these adsorption experiments for 1 day at pH = 6.0, $T = 298 \text{ K}$, and with 100 mg L^{-1} of methyl orange concentration (initial). Results show that polyaniline improves the blend membrane's adsorption capacity by increasing its concentration due to its hydrophilic nature, large surface area, and porous structure on the surface of the developed membrane. Polyaniline also increases the interactions (hydrogen bonding and π - π attraction) between dye molecules and the membrane's surface to enhance the adsorption mechanism.^[47] Figure 6b shows the effect of adsorption efficiency of methyl orange with change in concentration (0.5–4 g L^{-1}) of

the developed membrane (3P) for the same interval of time (3 h). Results show that adsorption efficiency gradually increases the concentration of 3P membranes (adsorbent) due to the increased number of active sites for dye molecules' adsorption on the membrane surface. Figure 6c shows the pH effect on adsorption efficiency of the developed membrane. The capacity of methyl orange adsorption greatly influences the change in pH from 4.5 to 11.5. At low pH (4.5–6.5), the adsorption of dye molecules gradually increased. However, with the further increase in pH value (6.5–11.5), the rate of adsorption gradually decreased due to the presence of hydroxyl ions (negative) on the membrane surface, which create repulsion between the membrane's surface and dye molecules.^[48] The pH value of permeate solution directly affects the functional group (such as the amine group) present on the developed membrane's surface.^[49] At low pH, amine groups are protonated, which increases the electrostatic force of attractions between membrane and dye molecules. When we further increase the pH value, these functional groups are deprotonated, which increases the repulsion between the dye molecule and membrane surface. The adsorption capacity of the developed 3P membrane for the different time intervals is shown in Figure 6d. We divided this adsorption time into two distinct stages. During the first 11 h (first stage), the adsorption rate of the 3P membrane gradually increased over time and attained the adsorption equilibrium by occupying the active sites.^[50] In the second stage, the adsorption rate remains constant due to the unavailability of dye molecules' adsorption site and saturation effect on the membrane surface.

Table S3, Supporting Information, shows the adoption isotherm of dye adsorption through synthesized membranes. We analyzed our dye adsorption properties through Langmuir and Freundlich isotherm models. Table S3, Supporting Information, shows that the process of dye adsorption takes place on a monolayer, and the adsorption sites on the membrane surface are homogenous.^[51] Because the coefficient for the Langmuir isotherm model is 0.99698, which is larger than the Freundlich isotherm model (0.9869), we can explain the adsorption mechanism of methyl orange through the Langmuir isotherm model. The maximum adsorption capacity (q_m) of the dye molecule through 3P (PVDF/PANI) membrane is more significant than pure PVDF membrane. Values of $1/n$ (0.249) also indicate that the developed membrane's surface is suitable for dye adsorption on these conditions (membrane's weight = 4.5 g, pH = 6.5, temperature = 298 K). There are two criteria for the determination of the adsorption kinetics model on the composite membrane. The first criterion is the value of R^2 , and second criterion depends on the importance of adsorption capacity. The kinetics model is more favorable when the value of R^2 is higher, and the difference of value in adsorption capacity is more significant. We determine the kinetics of dyes adsorption based on correlation coefficient (R^2) and the difference in dye adsorption capacity between kinetics models and our experimental results. Table S4, Supporting Information, shows the different parameters and correlation coefficient (R^2) of the pseudo-first-order (PFO) model and pseudo-second-order model (PSO). Results show that PSO is more suitable for describing the kinetics of the dye adsorption process because the value of R^2 for PFO (0.9745) is smaller than that for PSO (0.9803). The value of q_e is also greater for PSO (398.4) than for PFO (298.6).

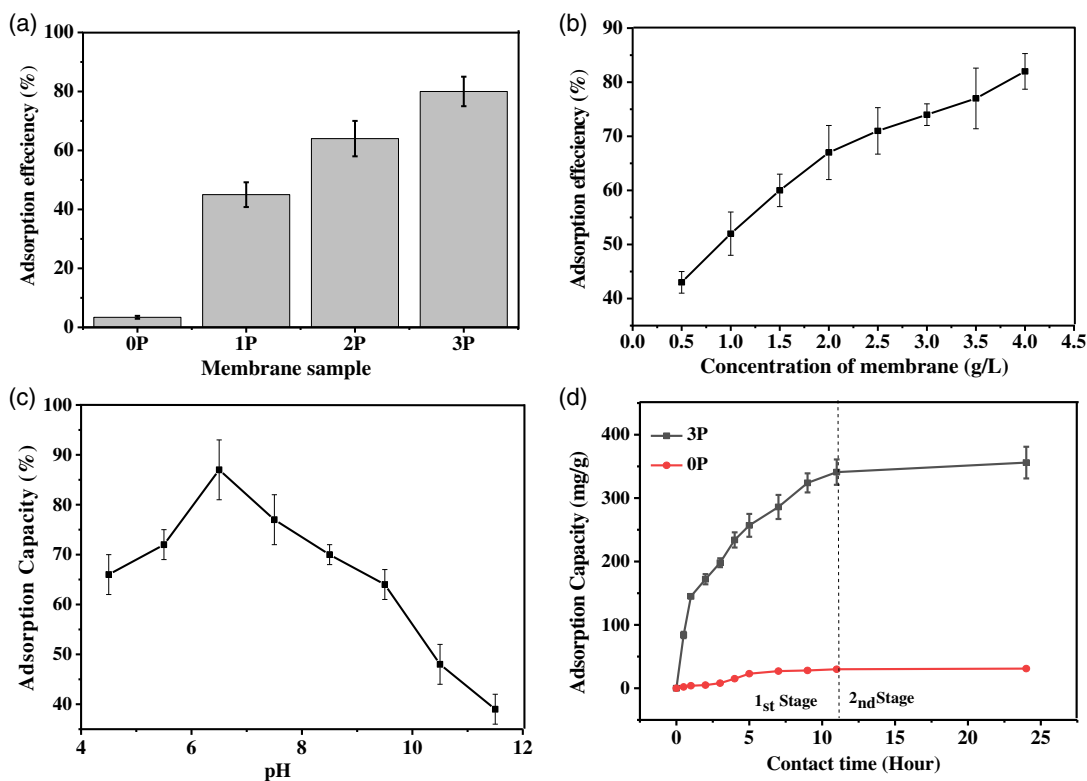


Figure 6. a) Adsorption capacity of synthesized membranes. b) Effect on adsorption efficiency with the change in concentration of the developed 3P membrane. c) Effect of pH on adsorption capacity. d) Capacity of dye adsorption for 24 h.

4.4.1. Practical Implications and Reusability Testing of Membranes

During the filtration process, dye flux of the membrane declined due to the penetration of different particles and solutes on the membrane's surface that caused membrane fouling.^[52] The fouling of membrane is unavoidable, but suitable strategies can be applied for reducing hydrophilic property in pure PVDF membranes. In this study, PANI was used as a hydrophilic additive to increase the membrane's hydrophilicity, improving its antifouling properties. Dye flux for a long time through synthesized membranes is shown in **Figure 7a**. The dye flux of the highly concentrated polyaniline membrane remained constant compared with other synthesized membranes due to the hydrophilic property of polyaniline in the hybrid membrane.^[53] To check the reusability of synthesized membranes, dye molecules (MO) in feed solution were used as the fouling agent. To remove these fouling agents, we washed these contaminated membranes with the solution of sodium hydroxide (0.05 M) for 30 min after each cycle, and then we again checked their filtration efficiency.^[54] BSA (model fouling agent) was used for checking the antifouling properties of the membrane. Pure water flux was measured before and after BSA solution filtration and described as fouling recovery ratio. **Figure 7b** shows that synthesized PVDF membranes were not sufficient for the rejection (39%) of BSA solution due to their hydrophobic nature. Polyaniline increases the hydrophilic properties (1P, 2P, and 3P) of developed membranes as the rates of BSA rejection improved to about 51%, 66%, and 71%, respectively.^[55] **Figure 7c** shows that after three different cycles,

the flux recovery ratio of hybrid membranes (1P, 2P, and 3P) is high compared with the neat PVDF membrane.

To check the developed membrane's recycling properties, we use different solutions to remove the contaminant from the developed membrane. Results in **Figure 7d** show that sodium hydroxide is more suitable for the desorption of methyl orange. This is due to the repulsive forces between dye molecules in an alkaline medium. **Figure 7e** shows the concentration effect of NaOH (sodium hydroxide). The process of desorption is high in a low concentration of sodium hydroxide. Na^+ ions may form the complex with dye molecules at a high concentration that decreases the process of desorption from the surface of blend membranes. For the evaluation of the developed PVDF/PANI membrane's stability, experiments were run to estimate the membrane's long-term performance. A water filtration test was conducted for 450 h at 0.1 MPa pressure.^[56] The dye flux and dye rejection were calculated after every 5 h. Rejection of dyes through sieving and adsorption mechanism is important for membrane stability and environmental conservation.^[57] Therefore, this hybrid membrane's long-term stability is high and can be easily cleaned after treating it with sodium hydroxide solution.^[58] The fouled membrane was washed with sodium hydroxide after 6 days. Results of dye flux and dye rejection of hybrid membrane are shown in **Figure 7f**. It was noted that dye flux slightly decreased to about 8% over time, but it recovered after being treated with HCl solution. Similar behavior was observed with dye rejection. The rate of dye rejection was dropped to about 6%, but it was also recovered to 96% after cleaning.

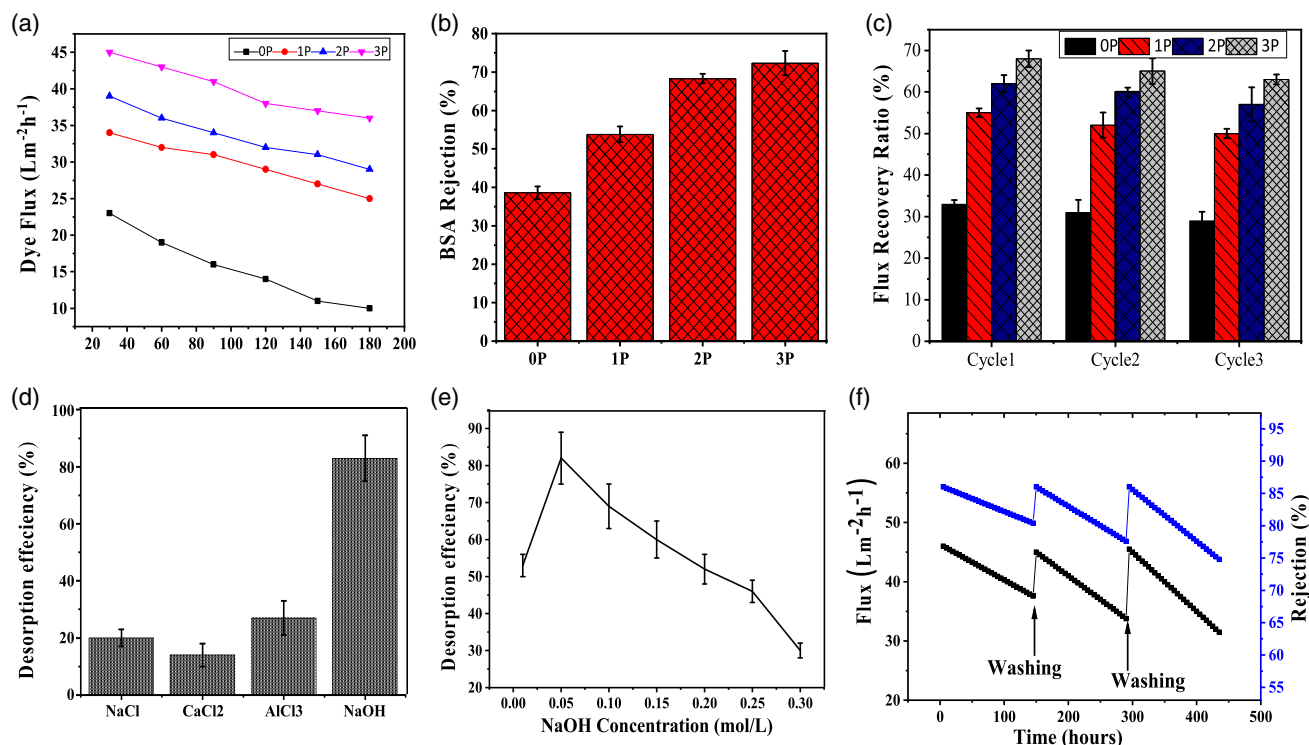


Figure 7. a) Dye flux of PVDF/PANI hybrid membranes for a long time. b) Rejection of BSA solution through PVDF/PANI hybrid membranes. c) Flux recovery ratio of PVDF/PANI hybrid membranes in each cycle. d) Desorption of methyl orange through different solutions. e) Effect of varying concentrations of NaOH on desorption efficiency. f) Reusability of PVDF/PANI hybrid membranes.

Results show that the composite PVDF/PANI hybrid membrane has excellent potential for removing the contaminants (dyes) from wastewater. We compared some significant parameters and their key results with the commercially available PVDF membrane to demonstrate the superior properties of the synthesized hybrid membrane in real wastewater treatment. Our results show that our synthesized membranes' contact angle was lower (46.11°) compared with the previously synthesized PVDF membrane (89°). Therefore, it shows the hydrophilic nature and excellent antifouling property.^[59] The pure water flux of commercial PVDF membranes ($25 \text{ L m}^{-2} \text{ h}$) was less than that of our novel synthesized membranes ($46 \text{ L m}^{-2} \text{ h}$).^[60] The membrane recycling test results indicate that the synthesized hybrid membrane contains long-term stability during the water filtration process. We can say that our synthesized membranes can provide a new route for a sustainable environment by removing hazardous contaminants from textile wastewater.

5. Conclusion

In this study, we investigated the properties and applicability of hybrid membrane based on poly(vinylidene fluoride)/polyaniline for the treatment of textile wastewater. The hybrid membranes were fabricated by addition of various concentrations of PANI into PVDF used the phase-inversion method. The presence of PANI was confirmed using different characterization techniques such as SEM, FTIR, and XRD. TGA analysis showed

better thermal stability of the hybrid membrane due to good interfacial interactions among PANI and PVDF, leading to increase in the degradation temperature. Experimental results indicated that membrane properties (pure water flux, solvent content, porosity, etc.) were improved with addition of polyaniline in the pure PVDF membrane. SEM analysis indicated that polyaniline not only improves the surface of membrane but also reduces the diameter of pores of the pure PVDF membranes from ≈ 1.53 to $0.78 \mu\text{m}$. Gradual decrease in contact angle represents that the polyaniline could effectively improve the hydrophilicity of pure PVDF membrane. The adsorption kinetics of methyl orange through developed membranes show that the results are well fitted in Langmuir's isotherm. The hybrid PVDF/PANI membrane also exhibits high rejections of methyl orange and allura red, about 81% and 85%, respectively. These results imply that PVDF/PANI hybrid membranes can be effectively used for the treatment of textile wastewater.

Supporting Information

Supporting Information is available from the Wiley Online Library or from the author.

Acknowledgements

Our research work was funded by Global Challenges Research Fund (GCRF), United Kingdom Research and Innovation, and The University of Manchester.

Conflict of Interest

The authors declare no conflict of interest.

Data Availability Statement

The data that supports the findings of this study are available in the supplementary material of this article.

Keywords

antifouling, phase inversions, polyaniline, polyvinylidene fluoride, ultrafiltration membranes

Received: June 8, 2021

Revised: August 5, 2021

Published online: September 12, 2021

- [1] R. Afroz, H. Banna, M. M. Masud, R. Akhtar, S. R. Yahaya, *Desalin. Water Treat.* **2016**, 57, 115.
- [2] N. Voulvoulis, K. Georges, in *Impact of Water Pollution on Human Health and Environmental Sustainability*, IGI Global, Hershey, PA **2016**, p. 29.
- [3] M. Papa, C. Alfonsín, M. T. Moreira, G. Bertanza, *J. Cleaner Prod.* **2016**, 113, 311.
- [4] R. Islam, J. Al Foisal, M. Rahman, L. A. Lisa, D. K. Paul, *Afr. J. Environ. Sci. Technol.* **2016**, 10, 9.
- [5] M. R. Bhuiyan, M. M. Rahman, A. Shaid, M. Bashar, M. A. Khan, *J. Cleaner Prod.* **2016**, 112, 3063.
- [6] L. A. Schaidler, K. M. Rodgers, R. A. Rudel, *Environ. Sci. Technol.* **2017**, 51, 7304.
- [7] F. S. Cesa, A. Turra, J. Baroque-Ramos, *Sci. Total Environ.* **2017**, 598, 1116.
- [8] B. Frindt, J. Mattusch, T. Reemtsma, A. G. Griesbeck, A. Rehorek, *Environ. Sci. Pollut. Res.* **2017**, 24, 10929.
- [9] M. Bilal, M. Asgher, R. Parra-Saldivar, H. Hu, W. Wang, X. Zhang, H. M. Iqbal, *Sci. Total Environ.* **2017**, 576, 646.
- [10] H. Wu, J. Mansouri, V. Chen, *J. Membr. Sci.* **2013**, 433, 135.
- [11] Q.-Z. Zheng, P. Wang, Y.-N. Yang, D.-J. Cui, *J. Membr. Sci.* **2006**, 286, 7.
- [12] L. Wu, J. Sun, Q. Wang, *J. Membr. Sci.* **2006**, 285, 290.
- [13] R. Malaisamy, R. Mahendran, D. Mohan, M. Rajendran, V. Mohan, *J. Appl. Polym. Sci.* **2002**, 86, 1749.
- [14] T. He, A. Bahi, W. Zhou, F. Ko, *J. Nanosci. Nanotechnol.* **2016**, 16, 7388.
- [15] C. Ong, W. Lau, B. Al-Anzi, A. Ismail, *Membr. Water Treat.* **2017**, 8, 211.
- [16] M. Lei, B. Xu, Y. Pei, H. Lu, Y. Q. Fu, *Soft Matter* **2016**, 12, 106.
- [17] L. Yan, Y. S. Li, C. B. Xiang, S. Xianda, *J. Membr. Sci.* **2006**, 276, 162.
- [18] A. Nasar, F. Mashkoor, *Environ. Sci. Pollut. Res.* **2019**, 26, 5333.
- [19] N. Khumalo, L. Nthunya, E. De Canck, S. Derese, A. Verliefde, A. Kuvarega, B. Mamba, S. Mhlanga, D. Dlamini, *Sep. Purif. Technol.* **2019**, 211, 578.
- [20] V. Dhand, S. K. Hong, L. Li, J.-M. Kim, S. H. Kim, K. Y. Rhee, H. W. Lee, *Compos. Part B: Eng.* **2019**, 160, 632.
- [21] G. Zeng, Z. Ye, Y. He, X. Yang, J. Ma, H. Shi, Z. Feng, *Chem. Eng. J.* **2017**, 323, 572.
- [22] E. N. Zare, A. Motahari, M. Sillanpää, *Environ. Res.* **2018**, 162, 173.
- [23] X.-L. Cao, Y.-N. Yan, F.-Y. Zhou, S.-P. Sun, *J. Membr. Sci.* **2020**, 595, 117476.
- [24] L. Yan, S. Hong, M. L. Li, Y. S. Li, *Sep. Purif. Technol.* **2009**, 66, 347.
- [25] O. Benhabiles, F. Galiano, T. Marino, H. Mahmoudi, H. Lounici, A. Figoli, *Molecules* **2019**, 24, 724.
- [26] R. Zhang, Y. Liu, M. He, Y. Su, X. Zhao, M. Elimelech, Z. Jiang, *Chem. Soc. Rev.* **2016**, 45, 5888.
- [27] S. Carretier, L.-A. Chen, A. Venault, Z.-R. Yang, P. Aimar, Y. Chang, *J. Membr. Sci.* **2016**, 510, 355.
- [28] S. Komarneni, R. Roy, Q. Li, *Mater. Res. Bull.* **1992**, 27, 1393.
- [29] V. G. Kulkarni, L. D. Campbell, W. R. Mathew, *Synth. Met.* **1989**, 30, 321.
- [30] M. Norouzi, M. Pakizeh, M. Namvar-Mahboub, *Desal. Water Treat.* **2016**, 57, 24778.
- [31] A. Behboudi, Y. Jafarzadeh, R. Yegani, *J. Membr. Sci.* **2017**, 534, 18.
- [32] G. Whyman, E. Bormashenko, T. Stein, *Chem. Phys. Lett.* **2008**, 450, 355.
- [33] S. Ayyaru, Y.-H. Ahn, *J. Membr. Sci.* **2017**, 525, 210.
- [34] M.-N. Huang, Z.-Q. Jiang, F.-B. Li, H. Yang, Z.-L. Xu, *New J. Chem.* **2017**, 41, 7544.
- [35] A. Mocanu, E. Rusen, A. Diacon, C. Damian, A. Dinescu, M. Suche, *J. Nanomater.* **2017**, 1, 401503.
- [36] E. Bet-Moushoul, Y. Mansourpanah, K. Farhadi, M. Tabatabaei, *Chem. Eng. J.* **2016**, 283, 29.
- [37] A. Ahmad, S. H. Mohd-Setapar, C. S. Chuong, A. Khatoon, W. A. Wani, R. Kumar, M. Rafatullah, *RSC Adv.* **2015**, 5, 30801.
- [38] S. Zinadini, A. A. Zinatizadeh, M. Rahimi, V. Vatanpour, H. Zangeneh, *J. Membr. Sci.* **2014**, 453, 292.
- [39] A. J. Kajakar, B. Dodamani, A. M. Isloor, Z. A. Karim, N. B. Cheer, A. Ismail, S. J. Shilton, *Desalination* **2015**, 365, 117.
- [40] R. Sharma, B. S. Kaith, S. Kalia, D. Pathania, A. Kumar, N. Sharma, R. M. Street, C. Schauer, *J. Environ. Manage.* **2015**, 162, 37.
- [41] J. Hester, A. Mayes, *J. Membr. Sci.* **2002**, 202, 119.
- [42] I. Koyuncu, D. Topacik, M. R. Wiesner, *Water Res.* **2004**, 38, 432.
- [43] W. Li, H.-L. Wang, *J. Am. Chem. Soc.* **2004**, 126, 2278.
- [44] S. J. Oh, N. Kim, Y. T. Lee, *J. Membr. Sci.* **2009**, 345, 13.
- [45] R. Gopal, S. Kaur, Z. Ma, C. Chan, S. Ramakrishna, T. Matsuura, *J. Membr. Sci.* **2006**, 281, 581.
- [46] S. Boributh, A. Chanachai, R. Jiraratananon, *J. Membr. Sci.* **2009**, 342, 97.
- [47] M. Hasan, M. M. Rashid, M. M. Hossain, M. K. Al Mesfer, M. Arshad, M. Danish, M. Lee, A. El Jerry, N. Kumar, *Polymer Testing* **2019**, 77, 105909.
- [48] S. M. Ahmed, F. I. El-Dib, N. S. El-Gendy, W. M. Sayed, M. El-Khodary, *Arab. J. Chem.* **2016**, 9, S1721.
- [49] H. N. Bhatti, Z. Mahmood, A. Kausar, S. M. Yakout, O. H. Shair, M. Iqbal, *Int. J. Biol. Macromol.* **2020**, 153, 146.
- [50] B. Goswami, D. Mahanta, *J. Environ. Chem. Eng.* **2020**, 8, 103919.
- [51] F. Ishtiaq, H. N. Bhatti, A. Khan, M. Iqbal, A. Kausar, *Int. J. Biol. Macromol.* **2020**, 147, 217.
- [52] M. Isoyama, S.-I. Wada, *J. Hazard. Mater.* **2007**, 143, 636.
- [53] C. Zhao, X. Xu, J. Chen, F. Yang, *J. Environ. Chem. Eng.* **2013**, 1, 349.
- [54] X. Chen, G. Huang, C. An, R. Feng, Y. Wu, C. Huang, *J. Membr. Sci.* **2019**, 582, 70.
- [55] A. K. An, J. Guo, E.-J. Lee, S. Jeong, Y. Zhao, Z. Wang, T. Leiknes, *J. Membr. Sci.* **2017**, 525, 57.
- [56] T. Inaba, T. Aoyagi, T. Hori, A. Charfi, C. Suh, J. H. Lee, Y. Sato, A. Ogata, H. Aizawa, H. Habe, *Biochem. Eng. J.* **2020**, 154, 107461.
- [57] A. Alammar, S.-H. Park, C. J. Williams, B. Derby, G. Szekely, *J. Membr. Sci.* **2020**, 603, 118007.
- [58] G. Balcioglu, G. Yilmaz, Z. B. Gonder, *Chem. Eng. J.* **2020**, 404, 126261.
- [59] H. Yu, L. Gu, S. Wu, G. Dong, X. Qiao, K. Zhang, X. Lu, H. Wen, D. Zhang, *Sep. Purif. Technol.* **2020**, 247, 116889.
- [60] S. Ayyaru, T. T. L. Dinh, Y.-H. Ahn, *Chemosphere* **2020**, 241, 125068.